Biomaterials 275 (2021) 120912

Contents lists available at ScienceDirect

Biomaterials

journal homepage: www.elsevier.com/locate/biomaterials

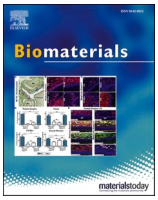

Cell-free, quantitative mineralization measurements as a proxy to identify osteoinductive bone graft substitutes

Yassine Maazouz, Giacomo Chizzola, Nicola Döbelin, Marc Bohner *

RMS Foundation, Bischmattstrasse 12, 2544, Bettlach, Switzerland

ARTICLE INFO

Keywords:
Osteoinduction
Bone graft substitutes
Calcium phosphate
Mineralization
In vitro
In vivo
Ectopic bone formation
Heterotopic ossification

ABSTRACT

Some synthetic bone graft substitutes (BGS) can trigger ectopic bone formation, which is the hallmark of osteoinduction and the most important prerequisite for the repair of large bone defects. Unfortunately, measuring or predicting BGS osteoinductive potential based on in vitro experiments is currently impossible. A recent study claimed that synthetic BGS can induce bone formation ectopically if they create a local homeostatic imbalance during their in vivo mineralization. This raised the hope that a simple cell free in vitro mineralization experiment would correlate with osteoinduction. The aim of the present study was therefore to assess the ability of a quantitative in vitro mineralization test to predict and rank the osteoinductive potential of BGS. Eight calcium phosphate BGS already tested ectopically in 9 different in vivo studies were used for that purpose. The experiment was able to identify materials that are reliably osteoinductive from those that are not, but was inaccurate in ranking the osteoinductive materials between each other. Chemical contaminants (Ca^{2+}, Mg^{2+}, H^{+}, OH^{-}, PO_4^{3-}) present in some of the BGS affected the in vitro mineralization experiment results, but not in a direction that could explain the different rankings. In conclusion, this study suggests that an in vitro experiment can be used as a fast and reliable screening tool to identify osteoinductive BGS and underline the need to study ionic contaminants on calcium phosphate BGS.

1. Introduction

Large bone defects remain a particularly challenging condition to treat. Existing options include bone grafts, their substitutes, orthobiologics and surgical techniques, but the vast majority of procedures are still treated with autografts, mostly due to their osteoinductive property. Although the definition of osteoinduction does not make a complete consensus, it is generally accepted that it is the process by which osteogenesis is induced in non-osseous sites [1]. This property is tested in vivo by implanting bone grafts substitutes (BGS) in a soft tissue, typically under the skin or in a muscle.

Synthetic bone graft substitute materials are seldomly used in the treatment of large bone defects [2] because they are considered to be non-osteoinductive, thus inferior to autologous bone grafts [3]. Nevertheless, some biomaterials including metals, polymers and ceramics have demonstrated reproducibly the ability to trigger bone formation ectopically [4–6]. The mechanism has remained elusive [1,7], but a large enough porosity [8], a high specific surface area [9,10], and a sub micrometric topography [11–13] have been shown to positively affect the osteoinductive potential of synthetic BGS. Besides, the ability of materials to become coated with a calcium phosphate layer once implanted in vivo, the so-called "bioactivity" [14,15], has been associated with the osteoinduction of metals [16–18], polymers [19,20] and ceramics [21,22]. Accordingly, calcium phosphates constitute the bone graft substitute (BGS) family that most consistently exhibits an osteoinductive action [1,23].

The various mechanisms that have been proposed to explain how a material can induce bone formation ectopically have failed to explain why bone forms first in the centre of the implanted material [24]. Invoking physical-chemical aspects that are the same in the inner and outer surfaces, such as porosity, SSA, pore size, or topography, does not provide a convincing explanation. In fact, the formation of bone in the core of the implant suggests a diffusion aspect, as pointed out by Habibovic et al. [25]. This was taken into account in a recent mechanism [26] which proposed that materials may consume more calcium and phosphate ions during their in vivo mineralization than the biologically supplied amounts, thus creating a homeostatic imbalance and the formation of sub-physiological calcium and phosphate concentrations. This

* Corresponding author. RMS Foundation, Bischmattstrasse 12, CH-2544, Bettlach, Switzerland.
E-mail address: marc.bohner@rms-foundation.ch (M. Bohner).

https://doi.org/10.1016/j.biomaterials.2021.120912
Received 14 October 2020; Received in revised form 5 May 2021; Accepted 20 May 2021
Available online 28 May 2021

condition was claimed to be the trigger for the initiation of the host tissue response leading to ectopic bone formation [26]. This concept represents a paradigm shift since this proposed mechanism of osteoinduction is not biologically- but chemically driven, and there is no release but an uptake of soluble factors.

The mechanism of Bohner and Miron [26], which only involves a physicochemical phenomenon, provides a great opportunity to design an in vitro test. The ISO 23317:2014 standard test method used to assess the mineralization ability of materials is only qualitative and takes 4 weeks [27,28]. So, a new quantitative approach was proposed and used to measure the mineralization of different types of β-TCP varying in composition, sintering temperature, microporosity and granule size [29]. A strong correlation was found between the mineralization ability and the different physical properties of β-TCP identified in the literature as strongly influencing the osteoinductive potential. Despite these positive results, the biological relevance of the experiment remains unclear.

Many considerations have propelled researchers to elaborate in vitro tests to avoid animal studies in agreement with the 3Rs principles [30,31]. Most of the tests consist in cellular cultures in direct contact or in liquid extracts of the bone graft substitutes [32,33]. Primary mesenchymal stromal cells or preosteoblast cell lines are generally used in single culture tests. Some more elaborate systems employ co-cultures of different cell types [34]. Unfortunately, these systems fail to encompass the biological complexity occurring in vivo [34]. Accordingly, Hulsart-Bilstrom et al. [35] found a very poor correlation between in vivo and in vitro behaviour of bone graft substitutes in a multicentre study. Others have even found inverse correlations between osteoinduction and proliferation of cells in vitro [10]. Thus in vitro cellular testing is not a predictive tool for osteoinduction due to false positives and false negatives [34].

This study aimed at testing the hypothesis that the in vitro experiment proposed in Ref. [29] can predict the osteoinductive potential of calcium phosphate BGS. Eight different BGS provided by Kuros Biosciences BV were considered for that purpose. These materials were tested in 9 different in vivo studies performed by 3 distinct teams in 3 different countries involving 3 large animal species [9,11–13,25,36–39]. Only ectopic implantations of these materials were considered, since it is the standard procedure to evaluate osteoinduction [1]. The materials were submitted to the mineralization test proposed in Ref. [29]. Subsequently, their in vivo osteoinductive potential was compared with their in vitro predicted potential with the aim to correlate mineralization ability and osteoinduction.

2. Materials and methods

2.1. Study protocol

The tested materials were synthesized by Kuros Biosciences BV. Their in vivo performance was assessed in animal studies and published in different research articles (Table 1). The materials were then tested for their mineralization potential at RMS Foundation. The materials were provided to RMS Foundation as pseudonymized samples numbered from M01 to M08). RMS Foundation did not know, nor attempted to know the nature of the composition or any other details on the materials

Table 1
Results of the different studies found in the literature on the ectopic implantation of the materials provided by Kuros Biosciences BV. Ø = diameter; H = height; w = week.

Author	Year	Animal model	Animal Number	Site of implantation	Materials used	Implant shape	Implant dimensions	Post implantation time	Bone occurrence	
									Time point 1	Time point 2
Yang [36]	1996	rat	10	Leg muscle/ abdomen skin	BCP1250/ M07	Cylinders	Ø2 x H3mm	6.5, 17 w	0	0
		rabbit	6	Dorsal muscle/ abdomen skin	BCP1250/ M07	Cylinders	Ø3 x H3mm	6.5, 17 w	0	0
		dog	4	Dorsal muscle/ abdomen skin	BCP1250/ M07	Cylinders	Ø4 x H3mm	6.5, 17 w	some	all
		pig	2	Dorsal muscle/ abdomen skin	BCP1250/ M07	Cylinders	Ø4 x H4mm	6.5, 17 w	some	all
		goat	2	Dorsal muscle/ abdomen skin	BCP1250/ M07	Cylinders	Ø4 x H5mm	6.5, 17 w	0	0
Yang [37]	1997	dog	4	Dorsal muscle	BCP1250/ M07	Cylinders	Ø4 x H5mm	6.5, 17 w	some	all
Habibovic [25]	2005	Dutch milk goats	10	Dorsal muscle	HA1150/ M05	Cylinders	Ø5 x H10mm	6w,12w	5/10	7/10
					BCP1150/ M03				7/10	6/10
Yuan [38]	2010	goat	10	Dorsal muscle	BCP1150/ M03	Granules	1–2 mm	12w	all	
					BCP1300/ M04				all	
					HA1300/ M06				None	
Zhang [9]	2014	dog	8	Dorsal muscle	TCP-B/M01	Granules	1–2 mm	12w	0/8	
					TCP-S/M02				8/8	
Davison [12]	2014	dog	8	Dorsal muscle	TCP-B/M01	Cylinders	Ø7 x H10mm	12w	0/8	
					TCP-S/M02				8/8	
Davison [39]	2015	dog	5	Dorsal muscle	BCP1150/ M03	Cylinders	Ø9 x H10mm	12w	4/5	
					BCP1300/ M04		Ø9 x H10mm		0/5	
Duan [11]	2016	dog	8	Dorsal muscle	TCP-B/M01	Granules	1–2 mm	12w	0/8	
					TCP-S/M02				8/8	
Duan [13]	2019	dog	8	Dorsal muscle	$BCP_{<\mu m}$/ M08	Granules	1–2 mm	12w	8/8	
					$TCP_{<\mu m}$/ M02				8/8	
					$TCP_{\mu m}$/M01				0/8	

before and during the in vitro mineralization and leachable experiments (in simulated body fluid (SBF) and demineralized water). After the experiments were performed, a meeting was set where Kuros Biosciences and RMS Foundation exchanged their results. RMS foundation posteriorly performed the physicochemical analysis of the materials.

2.2. Materials synthesis

The synthesis processes of the BGS provided by Kuros Biosciences are described in the published studies referenced in Table 1. Briefly, HA ceramics were prepared from HA powder (Merck) using the dual-phase mixing method and sintered at 1150 °C (M05) or 1300 °C (M06) for 8 h according to a previously described method [38]. Biphasic calcium phosphate (BCP) ceramics were fabricated using the H_2O_2 method using in-house made calcium-deficient hydroxyapatite (CDHA) powder and sintered at 1150 °C (M03), 1250 °C (M07) and 1300 °C (M04), respectively [36,38]. M08 was obtained from a BCP ceramic sintered at 1125 °C followed by hydrothermal treatment. Two types of CDHA powders were synthesized by adding a phosphoric acid solution (H_3PO_4, Fluka, Steinheim, Germany) to a calcium hydroxide suspension ($Ca(OH)_2$, Fluka) at different rates. To obtain M01, the calculated volume of phosphoric acid solution was directly poured into the calcium hydroxide suspension. Conversely, to prepare M02, the addition was performed dropwise. After aging at room temperature for 6 weeks, the CDHA slurries were filtered, dried, and grinded. The obtained CDHA powders were foamed by adding diluted H_2O_2 (1% in distilled water, Merck, Darmstadt, Germany) and a porogen (wax particles, 600–1000 μm, Merck) at 60 °C. M02 and M01 ceramics were then obtained by sintering the green bodies for 8h at 1050 °C and 1100 °C, respectively [9]. Ceramic particles (1–2 mm) were prepared by crushing and sieving (1–2 mm), cleaned ultrasonically with acetone and 70% ethanol, and finally dried at 80 °C.

2.3. Material characterization

For crystalline phase analysis, three separate samples of each material were ground in isopropanol and dried under an infrared light overnight. The resulting powders were pressed in polymer holders. A diffractometer (D8 Advance, Bruker, AXS GmbH, Karlsruhe, Germany) was used in a theta-theta setup with Ni-filtered Cu-Kα irradiation. Samples were analysed between 10 and 100° (2θ) in steps of 0.02° with a dwelling of 0.25 s per step and a rotation speed of 80 rpm. To quantify the phase composition, Rietveld refinement was applied using a software (PROFEX, https://www.profex-xrd.org/) [40]. Crystalline models for HA, β-TCP and MgO were taken from PDF# 01-074-0565 [41], PDF# 04–008-8714 [42], and PDF No. 04-010-4039 [43], respectively. (Ca + Mg)/P molar ratio were calculated from the phase quantification data assuming that the Ca/P molar ratio of β-TCP of HA were 1.50 and 1.67, respectively, and adjusting with MgO content where applicable.

The chemical composition of the materials was determined by ICP-MS (Agilent 7700 × , Agilent Technologies, Japan). For that purpose, the materials were weighed and digested in a solution of ultrapure H_2O containing 3% HNO_3 (HNO_3, Trace SELECT, Sigma Aldrich, Switzerland), 2% HCl (HCl, Rotipuran Supra, Carl Roth, Switzerland), and 0.01% HF (HF, Trace SELECT Ultra, Sigma Aldrich, Switzerland). ^{44}Ca signals and ^{31}P signals were calibrated against a multi-element custom standard solution (SUISSE-39, Inorganic Ventures, USA). Calibration drifts were corrected according to the custom calcium/phosphorus standard measured after every 8 samples and according to a 1000 ppb internal In/Sc standard solution (Inorganic Ventures, USA) measured along with each sample. Finally, the mean values of three measurements per sample were calculated. For simplification, "phosphate concentration" will be used in place of "phosphorus" concentration further in the text.

The specific surface area (SSA) was determined in triplicates by nitrogen adsorption using the BET model (Gemini 2360, Micromeritics). Prior to testing, the granules had been pre-dried at 150 °C for 20 min.

The general appearance of the granules was assessed using an optical (Stereomicroscope, M205A, Leica) and an electronic microscope (field emission scanning electron microscope, SEM; Sigma 300, Zeiss). The samples for SEM imaging were obtained by gluing some granules with a carbon tape onto aluminium pins and subsequent coating with a 15 nm thick (CCU-010, Safematic) gold layer. The internal structure of the granules was observed on polished sections of resin-embedded granules using the back scattered mode of the SEM. To prevent charging, the samples were coated with a 15 nm carbon layer. Bulk microporosity was derived from the analysis of binarized (ImageJ, NIH) back scattered electron images (n = 3).

2.4. In vitro experiments

Three types of in vitro experiments were performed: two mineralization experiments and one leachable experiment. The two mineralization experiments were executed in simulated body fluid (SBF) at a solid/liquid (S/L) ratio of 1.5 mg/mL and 200 mg/mL, respectively. These experiments were called "diluted mineralization experiment" and "concentrated mineralization experiment". The "leachable experiment" was performed in demineralized water (Resistivity < 18.2 MΩ, TOC < 5 ppb) at a S/L ratio of 200 mg/mL.

2.4.1. Diluted mineralization experiment

An SBF solution containing sodium, chloride, calcium and phosphate ions was chosen as incubation solution as proposed in Ref. [29]. SBF solution was produced from two stock solutions, a calcium rich solution (SBF–A) and a phosphate rich solution (SBF–B). Prior to each mineralization test, the two solutions were mixed in equal volumes (Table 2).

Titrator units (Titrando 907, Metrohm) were used to measure the evolution of the pH value of the SBF solution. The electrode was an internal reference pH electrode with a temperature sensor (Unitrode, Metrohm). The pH was recorded in situ on a computer through a processing program (Tiamo, Metrohm) for periods of up to 48 h. For the experiments, 300 mg of material were weighed and placed in a 3-neck bottle filled with 200 mL of SBF. The solution pH was monitored every 2 s for 22 h under mild propeller agitation (Fig. 1a) as described in Ref. [29]. Experiments were conducted in triplicates in a controlled temperature environment at 22 °C ± 2 °C. Solution aliquots (1 mL) were retrieved after 0.08 h (3 min), 0.25 h, 0.75 h, 2.25 h, 6.75 h, 20.25 h, and 22 h. The solution aliquots were not replaced. Some evaporation (≈1 mL) occurred during the experiment. Additional experiments were performed to assess the effect of contaminants on the mineralization results of samples M05 and M08. For that purpose, both granule types were washed in distilled water under mild agitation at a S/L ratio of 6 mg/mL (300 mg in 50 mL). The supernatant was removed after 24h of incubation at room temperature and the still wet granules were used immediately.

2.4.2. Concentrated mineralization experiments

A second type of mineralization experiment was performed at a higher S/L ratio to assess the effect of contaminants on mineralization. For the purpose of these "concentrated mineralization experiments", 200 mg of material were placed in 1 mL of solution [29] (Fig. 1b).

Table 2
Ionic concentrations (expressed in mM) of the SBF used in the ISO standard 23317 and the SBF used in the present study as compared to blood.

	Na^+	K^+	Mg^{2+}	Ca^{2+}	Cl^-	HCO_3^-	HPO_4^{2-}	SO_4^{2-}
Blood [49]	142.0	5.0	1.5	2.5	103.0	27.0	1.0	0.5
ISO 23317 [27]	142.0	5.0	1.5	2.5	147.8	4.2	1.0	0.5
SBF-A	161.2			3.7	164.3			
SBF–B	161.2				164.3		2.1	
SBF	161.2			3.7	164.3		2.1	

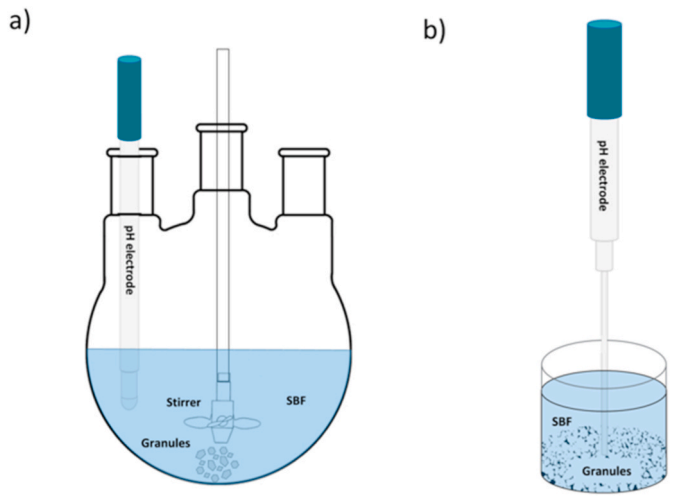

Fig. 1. a) Scheme of the diluted mineralization experiment conducted in a 3-neck bottle; 300 mg of BGS and 200 mL of SBF are agitated with a propeller during 22 h and the pH is monitored every 2 s; b) Schematic view of a single well of the concentrated mineralization experiment and the leachable experiment; tests are conducted in a 48-well plate; each well is filled with 200 mg of granules and either 1 mL of SBF or 1 mL of demineralized water, respectively.

Contrary to the diluted mineralization experiment, the pH value was not determined continuously, but at each of the 7 time points (5 min = 0.08 h, 0.25 h, 0.75 h, 2.25 h, 6.75 h, 20.25 h, 24 h). As each experiment was performed six times, 42 experiments were prepared for each material (7 time points x 6 repeats). The experiments were restricted to five materials: M01, M02, M03, M05, and M08. The pH value was measured with Titrator units (Titrando 907, Metrohm) using a miniaturized pH electrode for small volumes (Biotrode, Metrohm).

2.4.3. Leachable experiments

To assess the nature of the material contaminants, 200 mg of each of the tested materials (M01, M02, M03, M05, and M08) were incubated for 0.08 h, 0.25 h, 0.75 h, 2.25 h, 6.75 h, 20.25 h, and 24 h (7 time points) in 1 mL of pure water. Each experiment was performed six times, leading to a total of 42 samples per material. The pH value was measured with Titrator units (Titrando 907, Metrohm) using a miniaturized pH electrode for small volumes (Biotrode, Metrohm).

2.4.4. Chemical composition of the solutions

All solution aliquots were centrifuged for 2 min at 2000 rpm and the supernatant was filtered with nylon membrane filters of 0.2 μm (Rotilabo Nylon syringe filter, Carl Roth). The supernatants were then diluted 1:100 in a solution of ultrapure H_2O containing 3% HNO_3 (HNO_3, Trace SELECT, Sigma Aldrich, Switzerland), 2% HCl (HCl, Rotipuran Supra, Carl Roth, Switzerland), and 0.01% HF (HF, Trace SELECT Ultra, Sigma Aldrich, Switzerland). The solutions were analysed using ICP-MS (Agilent 7700 ×, Agilent Technologies, Japan). ^{44}Ca signals were calibrated against a certified single-element Ca standard (Karl Roth, Germany) and ^{31}P signals were calibrated against a multi-element standard solution (IV-ICPMS-71A, Inorganic Ventures, USA). Calibration drifts were corrected according to the calcium standard measured after every 8 samples and according to a 20 ppb internal In/Sc/Bi standard solution (Inorganic Ventures, USA) measured along with each sample. Finally, the mean values of three measurements per sample were determined.

2.5. Retrospective analysis of In vivo results

The in vivo ectopic implantation performed with the 8 materials provided by Kuros Biosciences were reviewed to identify the relative osteoinductive potential of the materials. Materials were classified as a function of the bone occurrence in the explants (all explants, some explants, none of the explants). Materials consistently exhibiting bone formation in all the explants were qualified as highly osteoinductive. Materials presenting bone occurrence in most but not all explants consistently in different studies were qualified as moderately osteoinductive. Materials that did not show any bone occurrence in some studies and exhibited some bone occurrence in at least one study were qualified as poorly osteoinductive. Finally, materials that consistently showed no bone formation were qualified as non-osteoinductive. For the purpose of constructing a binary response, highly and moderately osteoinductive BGS were qualified as reliably osteoinductive, while poorly and non-osteoinductive BGS were qualified as unreliably/non-osteoinductive.

2.6. Statistical analysis

Analysis of variance was performed with a software (Minitab 19, Minitab LLC), a confidence level of 99% was used and Dunnett's/Tukey's and Bonferroni's post hoc test were used to perform paired comparisons for one-way and two-way ANOVA respectively.

2.7. Correlation in vitro versus in vivo

The predictive capacity of the methods used was evaluated using the confusion matrix method [44]. The in vivo results were taken as the true class input and the results of the in vitro diluted mineralization experiment as the predicted class. Materials considered as true negatives (TN) and true positives (TP) were those that were identified as positives and as negatives in both true and predicted classes, respectively. Materials identified as false negatives (FN) were those, which were positives in vivo but negatives in vitro. Materials identified as false positives (FP) were those, which were negatives in vivo but positives in vitro. Sensitivity, specificity, precision, negative predictive value and accuracy were calculated for the diluted mineralization experiment as follows:

$$Sensitivity = \frac{TP}{TP + FN}$$

$$Specificity = \frac{TN}{FP + TN}$$

$$Precision = \frac{TP}{TP + FP}$$

$$Negative\ predictive\ value = \frac{TN}{TN + FN}$$

$$Accuracy = \frac{TP + TN}{TP + FN + FP + FN}$$

3. Results

3.1. Materials composition and properties

The materials were provided in granular form, sieved between 1 and 2 mm. Granules were similar in appearance, displaying irregularly shaped structures in the range of 1–2 mm (Fig. 2, left column). Granules seemed slightly smaller in the case of M02 and slightly larger in the case of M07. The materials M05, M06 and M07 had a light blue colour while the other materials were white. According to SEM images of the polished samples, intragranular macropores were present in all granule types (Fig. 2, centre left column). These intragranular macropores appeared less abundant in M03 and M04, and bimodally distributed in M08, but no systematic quantitative study was performed to enforce these statements. With the exception of M06 and M07, all samples were microporous (Fig. 2, centre right image). However, the microporosity of M04 seemed to be much lower than that of M01, M02, M03, M05, and M08.

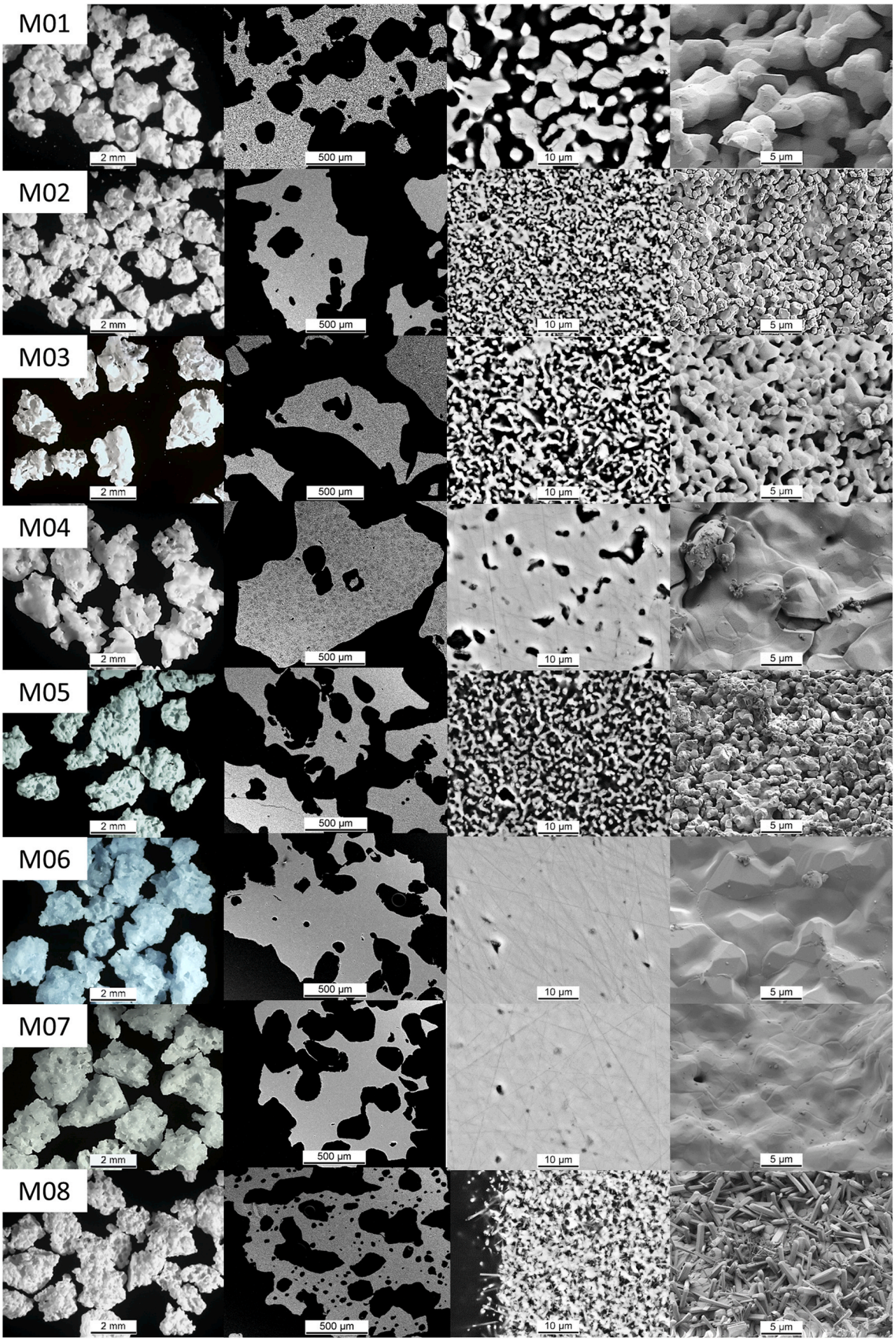

Fig. 2. Macro- and microstructure of the granules. Left column, optical microscopy images. Scanning electron microscope images (backscattered electrons) of polished resin embedded granules, centre-left macroscopic structure, centre-right microscopic structure of the bulk. Right column, scanning electron micrographs (secondary electrons) of the surface of the granules.

Among these materials, the micropores of M01 were markedly larger than those of materials M02, M03, M05 and M08. All materials but M08 presented the classical features of sintered ceramics with grains joined together to different degrees (Fig. 2, centre and right column). The grains were in the sub micrometric size range for M02, M03 and M05 while they were in the micrometric range in the case of M01, M04, M06 and M07. The surface of M08 granules consisted of a 10 μm thick layer of acicular hexagonal crystal.

The specific surface area (SSA, Fig. 3a) of the granules varied between 0.23 ± 0.01 m^2/g for M04 and 2.19 ± 0.01 m^2/g for M08. The materials M02, M03 and M05 had somewhat similar SSA but differed statistically. The rest of BGS had SSA inferior to 1 m^2/g. The impressions gained from the SEM images of polished samples (Fig. 2) were confirmed by microporosity measurements (Fig. 3b). Samples M01, M02, M03, M05 and M08 had a porosity close to 50% whereas samples M04, M06, and M07 were close to 10%.

Phase quantification results obtained by Rietveld refinement are presented in Fig. 3c. M02, M03, M04, M07 and M08 were found to consist of a mixture of β-TCP and HA (= BCP), with β-TCP as major component in M02, M07 and M08, and HA as major component in M03 and M04. M01 was phase pure β-TCP while M05 and M06 consisted of HA with a small percentage of magnesium oxide (0.24 ± 0.01 and 0.16 ± 0.02 wt% respectively).

The (Ca + Mg)/P ratios of the different materials determined by XRD could be compared with those calculated from ICP-MS results (Fig. 3d). Focusing first on the ICP-MS results, the (Ca + Mg)/P ratio was the highest for M05 and M06 with (1.676 ± 0.005 and 1.676 ± 0.011) and the lowest for M01 (1.497 ± 0.01). The (Ca + Mg)/P ratios determined by XRD were statistically equivalent (α = 0.01) to those determined by ICP-MS for all materials except for M08 (p = 0.007) for which the XRD method overestimated the ratio (1.561 ± 0.001 by XRD versus 1.522 ± 0.013 by ICP-MS). For comparison, Table 3 lists some of the material properties measured in the present study and published in the vivo studies.

3.2. In vivo studies

The results of the published in vivo studies are summarized in Table 1. M02 and M08 were shown to form bone in all ectopic implants used in the different studies in which they were analysed. They can consequently be classified as highly osteoinductive [9,11–13]. M05 and M03 were shown to induce ectopic bone formation in most but not all of the implants used in the studies focusing on them [25,38,39]. Their osteoinductive is most likely not as high as that of M02 and M08. M03 and M05 are considered to be moderately osteoinductive. M04 and M07 both showed bone formation in some studies and none in others [36–39], their osteoinductive potential is thus poor. Finally both M06 and M01 consistently failed to induce bone formation and therefore can be considered as being non osteoinductive [9,11,12,38]. Based on these findings, the materials M02, M08, M03 and M05 were classified as reliably osteoinductive and the materials M04, M07, M01 and M06 as unreliably/non-osteoinductive. A summary of the true osteoinductive potential classification obtained owing to this information is presented in Table 4.

3.3. In vitro experiments

In a previous study [29], a method to quantitatively assess mineralization in SBF of bone graft substitutes was designed. This method relies on the measurement of pH, calcium and phosphate as a proxy for the surface precipitation of a calcium phosphate in SBF. The same method was used in the present work. Nonetheless, the objective of the former study was different since the statistical analysis served to identify the bone graft substitutes' processing parameters and characteristics influence on the mineralization and the confinement. Here, the objective was to differentiate materials according to their mineralization capacity using paired comparison with a control. The responses analysed in the mineralization experiment were the pH decrease and the calcium and phosphate concentration decrease after 22h of incubation in SBF. Subsequently, in vitro and in vivo results were compared with the aim to find a correlation.

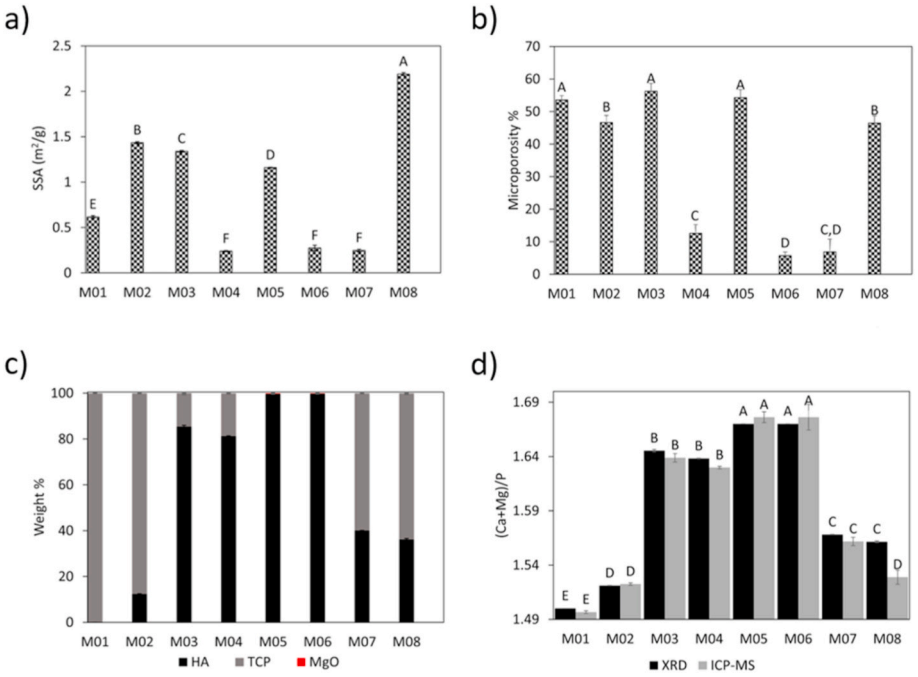

Fig. 3. Some physico-chemical properties of materials M01 to M08. a) Specific surface area; the labels indicate the statistically equivalent group as determined by Tukey's post hoc test (α = 0.01). b) Bulk microporosity. Error bars represent the standard deviation (n = 3). c) Phase composition as determined by XRD and Rietveld refinement. d) (Ca + Mg)/P ratio as determined by XRD and ICP-MS.

Table 3
Comparison between published and measured data for some of the properties of materials M01 to M08.

BGS	SSA (m^2/g)		Porosity (%)		Phase quantity (wt%)	
	Published	Measured	Published	Measured	Published	Measured
M01	0.7 [11],0.77 [12], 0.8 [9], 0.72 [13], 0.83 [21]	0.61 ± 0.01	Total:72 [9], 73 [11] Macro: 50 [11], 49 [9] Micro: 23 [11,13], 22 [9], 46.32 [21]	Micro: 54 ± 1	Pure β-TCP [9,11–13, 21]	Pure β-TCP
M02	1.4 [11], 1.47 [12], 1.2 [9], 1.71 [13], 1.85 [21]	1.43 ± 0.01	Total: 70 [9], 72 [11] Macro: 50 [11], 48 [9] Micro: 22 [9,11], 45.14 [21]	Micro: 47 ± 2	Pure β-TCP [9,11–13, 21]	β-TCP: 87.6 ± 0.1 HA: 12.2 ± 0.1
M03 [38]	1	1.33 ± 0.01	Total: Macro: Micro: 41.1	Micro: 56 ± 2	β-TCP: 20 HA: 80	β-TCP: 14.6 ± 0.5 HA: 85.4 ± 0.5
M04 [38]	0.2	0.23 ± 0.01	Total: Macro: Micro: 8.7	Micro: 13 ± 3	β-TCP: 20 HA: 80	β-TCP: 18.8 ± 0.2 HA: 81.2 ± 0.2
M05 [25]	1.32	1.16 ± 0.01	Total: Macro: 47.5 Micro:	Micro: 54 ± 2	Pure HA	HA: 99.76 ± 0.01 MgO: 0.24 ± 0.01
M06 [38]	0.1	0.27 ± 0.03	Total: Macro: 46.5 Micro: 3.1	Micro: 6 ± 1	Pure HA	HA: 99.84 ± 0.02 MgO: 0.16 ± 0.02
M07 [36, 37]	–	0.24 ± 0.01	Total: 61 Macro: Micro:	Micro: 7 ± 4	β-TCP: 63 HA: 37	β-TCP: 60.0 ± 0.1 HA: 40.0 ± 0.1
M08 [13]	2.77	2.19 ± 0.01	Total: Macro: Micro: 9	Micro: 46 ± 2	β-TCP: 75 HA: 25	β-TCP: 63.9 ± 0.4 HA: 36.1 ± 0.4

Table 4
Classification of BGS according to their observed osteoinductive capacity in vivo.

Osteoinductive potential	High	Moderate	Low	Null
Criteria of classification based on in vivo results	Bone occurrence in all explants in all studies	Bone occurrence in most explants in all studies	Bone occurrence in some explants in some studies	No bone occurrence
Eligible materials	M02, M08	M03, M05	M07, M04	M01, M06
Binary classification based on osteoinductivity reliability	Reliably osteoinductive		Unreliably/non osteoinductive	

3.3.1. Diluted mineralization experiments

In the diluted mineralization experiments, the pH decreased with time for all materials but M05 where the pH increased significantly ($p < 0.01$) before decreasing (Fig. 4a). For comparison, the pH of the SBF solution without any material in it slightly decreased as well. The pH results at 22 h were analysed statistically with the Dunett's post hoc test (CL 99%) using SBF as control. This paired comparison revealed that the solution pH was not affected by the addition of M04, M06, M07 and M01. In contrast, M02, M03, M05 and M08 all induced a pH decrease that differed statistically from that occurring in SBF alone (Table 5). Applying Tukey's post hoc test (CL 99%), the pH decrease was identified as being significantly greater for M03 followed by M08, and there was no difference between M02 and M05 (Table 6).

The calcium concentration (Fig. 4b) decreased with time for all materials. The phosphate concentration decreased for all materials except for M04, M06 and M07(Fig. 4b). The calcium and phosphate concentrations measured after 22 h were significantly lower for M02, M03, M05, and M08 than those of the control (SBF). This was not the case for M07, M04, M06 and M01 (Table 5). The exact ranking of the different materials when considering the drop of pH, calcium, and phosphate was determined applying the Tukey's post hoc test at a 99% confidence level and is presented in Table 6. When plotting the calcium and phosphate concentrations measured after 22 h of incubation for all materials, a linear correlation with a slope of 1.38 ± 0.08 ($R^2 = 0.987$) was found (Fig. 4d). The Ca/P molar ratio of the solution increased significantly after 22h of incubation for M02, M03 and M05 (Fig. 4c). It remained unchanged for M01, M04, M06, and M07, whereas it decreased in the case of M08.

3.3.2. Concentrated mineralization experiments

In the concentrated mineralization experiments, three groups could be identified with regards to the pH (Fig. 5a, Fig. S1b-S5b). M08 and M03 provoked a drop of pH in SBF (pH ≈ 6.2–6.0). M01 and M02 hardly modified the pH value (≈7.05–6.95). Finally, M05 increased markedly the pH value, up to ≈10. Calcium and phosphate concentrations decreased with time for M01, M02, M03 and M05 (Fig. 5b, Fig S1a-S5a). M05 experienced the largest decrease of both ions, down to 0.62 mM and 0.63 mM respectively, followed by M02. The materials M01 and M03 presented a similar evolution of the calcium and phosphate concentrations. In the case of M08, the calcium concentration experienced a slight decrease while phosphate experienced a net increase. These effects provoked large changes of the Ca/P of the solution (Fig. 5c, Fig. S1b-S5b), which increased to 10 for M05, to 7 for M02, and to 2–2.5 for M02 and M03. Contrarily, the Ca/P molar ratio of the solution decreased to 1.21 with M08. The higher S/L ratio in the concentrated mineralization experiments caused much larger compositional changes than in the diluted mineralization experiments (Figs. 4d and 5d).

3.3.3. Leachable experiments

Granules incubated in water induced larger pH variations than in SBF (Figs. 5a and 6a), even though similar trends were observed. M05 provoked a pH increase exceeding 3.5 pH units (≈10.5). M01 and M02 also made the water alkaline with pH variations above 2 pH units. M03 was the material that affected the pH the least with only 0.7–0.8 pH units. M08 was found to be acidic, dropping the pH by close to 0.9 units

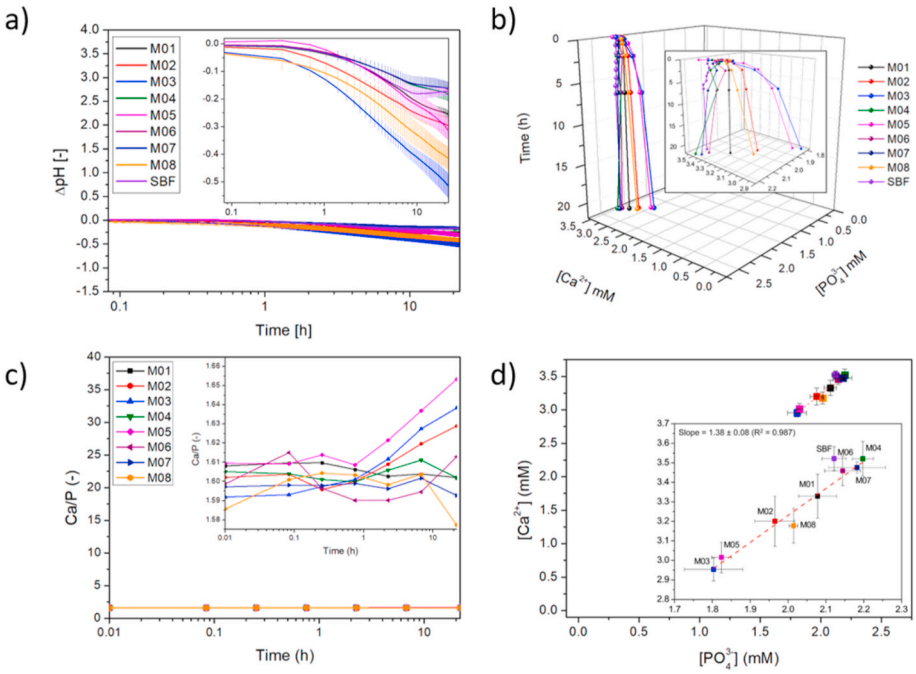

Fig. 4. Results of the diluted mineralization experiment. a) pH evolution. b) Evolution of the calcium and phosphate concentrations. c) Evolution of the Ca/P molar ratio of the solution. d) Linear regression performed on the calcium versus phosphate concentrations after 22h of incubation. Error bars represent the standard deviation (n = 3). The inserts show an enlargement of the results.

Table 5
Confusion matrix determined with the Dunnett's post hoc test correlating the true osteoinductivity (in vivo) with the different responses analysed in the diluted mineralization experiment (in vitro), namely pH, calcium, and phosphate (all at 22h). The test was negative at α = 0.01 if the drop of pH, calcium, or phosphate measured with one material at 22 h of reaction was not different from the drop measured with SBF alone. The test was positive α = 0.01 if the drop of pH, calcium, or phosphate measured with one material at 22 h of reaction was significantly larger than the drop measured with SBF alone. True positives and negatives are highlighted in green, false positives and negatives are highlighted in orange. Since the overall results were the same for pH, calcium and phosphate, one table is shown for all three measurables.

pH, Ca, PO_4^{3-}		In vivo	
		Negative	Positive
In vitro	Negative	M01, M06, M04, M07	None
	Positive	None	M02, M03, M05, M08

Table 6
Summary of the different rankings obtained according to physicochemical, in vitro and in vivo responses measured on the 8 different BGS. The rankings were obtained by applying the Tukey's post hoc test with a 99% confidence level.

Test	Response	Ranking
In vivo	Bone occurrence	M02 ≈ M08 > M03 ≈ M05 > M07 ≈ M04 > M01 ≈ M06
Physicochemical features	SSA	M08 > M02 > M03 > M05 > M01 > M04 ≈ M06 ≈ M07
	Bulk microporosity	M01 ≈ M03 ≈ M05 > M08 ≈ M02 > M04 ≥ M07 ≥ M06
	Ca + Mg/P	M05 ≈ M06 > M03 ≈ M04 > M07 > M02 ≈ M08 > M01
Mineralization	ΔpH(22h)	M03 > M08 > M02 ≈ M05 > SBF ≈ M01 ≈ M04 ≈ M06 ≈ M07
	[Ca](22h)	M03 > M05 > M08 > M02 > SBF ≈ M01 ≈ M04 ≈ M06 ≈ M07
	[P](22h)	M03 > M05 > M08 > M02 > SBF ≈ M01 ≈ M04 ≈ M06 ≈ M07

(≈6.1; Fig. S1d-S5d). Calcium and phosphate concentrations (Fig. 6b, Fig. S1c-S5c) slightly increased with time for all materials but more markedly in the case of M08 (Calcium up to 1.45 mM, phosphate up to 0.81 mM). The Ca/P of the solution (Fig. 6c, Fig. S1d-S5d) increased for all materials but M08 where it stabilized at a value of 0.57. For M01, the Ca/P molar ratio climbed to values over 40, not much higher than the value measured for M02 (>30). The changes of calcium and phosphate concentrations provoked by the materials in water were in general much more limited that those recorded in SBF with the exception of M08 (Figs. 5d and 6d).

3.3.4. *Diluted mineralization experiments with washed granules*

M05 and M08 granules were washed and tested in the diluted mineralization experiment. The effect of washing was different for M05 and M08 in that it increased the pH drop for M05 and reduced it for M08 (Fig. 7a and b). Both the calcium and phosphate concentration changes were smaller after washing both materials (Fig. 7c).

3.4. *Comparison of the in vitro and in vivo experiments*

The 4 materials (M02, M03, M05, and M08) that triggered a significantly different response than the control (SBF) were also the 4 materials that were reliably osteoinductive (Tables 4 and 5). This means that the in vitro experiment had no false positives or false negatives and accordingly, that the sensitivity and specificity reached 100% (Table 7). However, the material ranking was not the same in the in vitro experiment and the in vivo studies (Table 6).

4. Discussion

The aim of this study was to test the hypothesis that an in vitro mineralization experiment can be used to predict the in vivo osteoinductive potential of BGS. For that purpose, RMS Foundation tested blindly 8 different types of BGS provided by Kuros Biosciences. These 8 BGS had been tested for their osteoinductive potential in 9 different in vivo studies performed by 3 distinct teams in 3 different countries

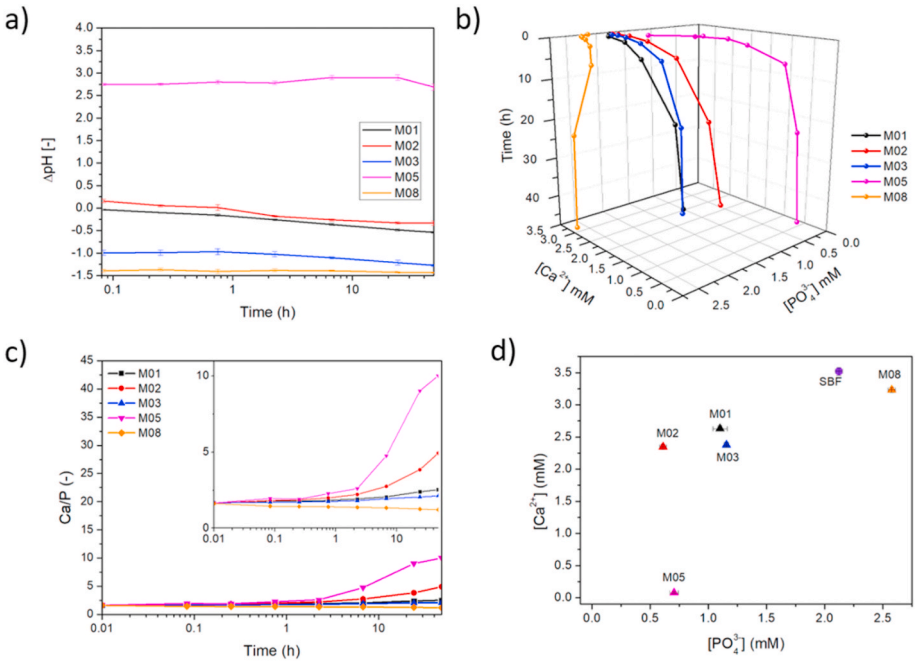

Fig. 5. Results of the concentrated mineralization experiment. a) pH evolution. b) Evolution of the calcium and phosphate concentrations. c) Evolution of the Ca/P molar ratio of the solution. d) Calcium and phosphate concentrations after 22h of incubation. Error bars represent the standard deviation (n = 6). The insert in c) shows an enlargement of the results.

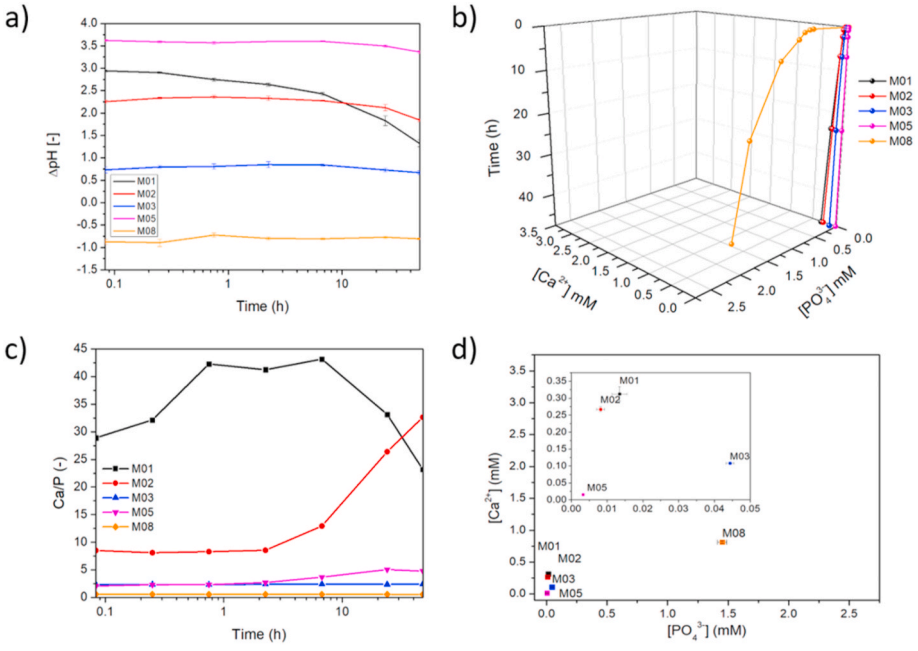

Fig. 6. Results of the leachable experiment in H_2O during 48h. a) pH evolution. b) Evolution of calcium and phosphate concentrations. c) Evolution of the Ca/P molar ratio of the solution. d) Calcium and phosphate concentration after 22h of incubation. Error bars represent the standard deviation (n = 6). The insert in d) shows an enlargement of the results.

involving 3 large animal species. Only ectopic implantations of these materials were considered, since it is the standard procedure to evaluate osteoinduction [1]. By applying the same method as in a previous study [29], a prediction of their osteoinductive potential by the in vitro experiment was obtained and the correlation with the in vivo results was evaluated.

The BGS provided by Kuros Biosciences did not proceed from the same batch as that used in the in vivo studies. Notwithstanding the BGS were produced using the same processes that were used for those studied in vivo. The comparison between the present material analysis and published data showed some discrepancies (Table 3). Some of these differences can be explained by batch-to-batch differences, for example for the SSA values. Other differences are more puzzling. For example, M02 is supposed to be pure β-TCP, but the XRD analysis revealed the presence of 12.2 ± 0.1% HA. A difference of 11% was also seen in the HA content of M08 (here: 36.1 ± 0.1% HA; published: 25% HA). The porosity data is the most difficult property to compare since different characterization methods were used within the published data and the

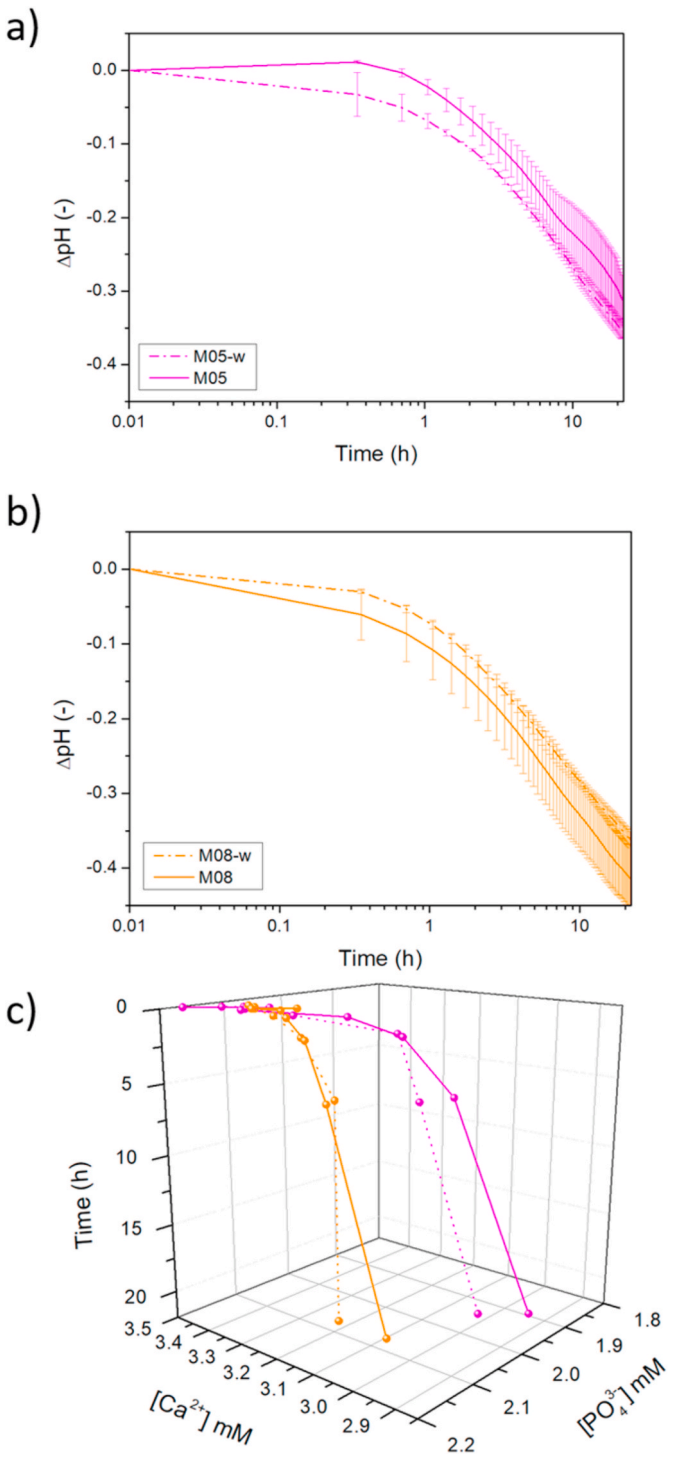

Fig. 7. Results of the diluted mineralization experiment obtained with unwashed and washed materials M05 and M08. a) pH evolution with unwashed and washed M05 ("M05" and "M05-w"). b) pH evolution with unwashed and washed M08 ("M08" and "M08-w"). c) Evolution of calcium and phosphate concentrations for unwashed and washed M05 and M08 granules. Error bars represent the standard deviation (n = 3).

present data. However, the microporosity results of the two most investigated materials (M01 and M02) seem to fit quite well. Indeed, the published microporosity measured by mercury porosimetry was close to 46% for M01 and M02, not far from the 54 ± 1 and 47 ± 2% measured here.

Most BGS were tested in at least 2 different in vivo studies (M01, M02, M03, M04, and M07), but some materials were studied only once ectopically (M05, M06, and M08). Furthermore, the materials that displayed the most reliable osteoinductive behaviour (M02, M03, M05 and M08) were not compared all together in the same study. For instance, M03 and M05 were tested together but neither M02 nor M08 were compared with them. Nonetheless, M02 and M08 were compared together. Therefore, it is not realistic to establish a perfectly accurate ranking between the materials that exhibited a reliable osteoinductive behaviour from the least to the most osteoinductive by interpreting the results published in the literature. This explains why the 4 classes considered with a moderated level of confidence (highly, moderately, poorly, non-osteoinductive) were reduced to only 2 classes ("reliably" versus "unreliably/non osteoinductive" (Table 4)) with a higher level of confidence.

Table 7
Prediction quality as calculated for the 3 responses analysed in the mineralization test owing to the confusion matrix method.

Responses of the mineralization test	ΔpH (22h)	[Ca] (22h)	[P] (22h)
True positives	4	4	4
True negatives	4	4	4
False Positives	0	0	0
False negatives	0	0	0
Sensitivity	100%	100%	100%
Specificity	100%	100%	100%
Positive predictive value	100%	100%	100%
Negative predictive value	100%	100%	100%
Accuracy	100%	100%	100%

The predictive metrics obtained by the confusion matrix method indicate that the mineralization experiment was capable of identifying the materials that were reliably osteoinductive (highly, M02 and M08; and moderate, M03 and M05). The experiment was also accurate at predicting the unreliably or non-osteoinductive feature of M06, M07, M04 and M01. The quantitative mineralization experiment achieved 100% accuracy, sensitivity, precision and specificity (Table 7). However, the mineralization experiment was not able to obtain the exact same order as that established with the in vivo results (Tables 4 and 6). It might be because the order obtained for reliably osteoinductive BGS from in vivo studies does not come from a direct in vivo comparison between M02, M08, M03 and M05 but from different studies combined. It might also be due to the effects of artefacts in the mineralization test, for example due to surface contaminants.

A recent in vivo study performed with M01 and M02 has shown that the biological response of M01 and M02 already differs after 24 h of implantation [45]. This could mean that rapidly dissolving surface contaminants could affect the in vivo behaviour of BGS. To investigate the possible influence of contaminants (traces of alkaline or acidic substances) on the outcome of the experiments, the S/L ratio was increased to 200 mg/mL (Fig. 1b), and incubation experiments were performed during 48h in SBF ("concentrated mineralization experiment"; Fig. 5) and in demineralized water ("leachable experiment"; Fig. 6). M05 was found to be alkaline and M08 acidic in both SBF and water (Figs. 5a and 6a) suggesting the presence of alkaline and acidic contaminants, respectively. M01 and M02 presented an alkaline behaviour in demineralized water, but not in SBF. The Ca/P of the incubated solution in the leachable study was superior to 20 for both M01 and M02, which is compatible with traces of a soluble calcium rich alkaline substance, possibly CaO, $Ca(OH)_2$, or $CaCO_3$ [29,46]. M05 released a Mg rich alkaline substance (Fig. S6), consistently with the presence of MgO identified by XRD (Fig. 3a). For M08, the Ca/P ratio of the solution decreased in both SBF (1.21) (Fig. 5c) and demineralized water (0.57) (Fig. 6c), suggesting a contamination with an acidic, phosphate rich substance (i.e. monocalcium phosphate monohydrate, $Ca(H_2PO_4)_2{\cdot}H_2O$). The presence of this contaminant explains why M08 released substantially larger amounts of calcium and phosphate than the rest of the tested BGS. The removal of contaminants in M05 and M08 (by

washing in demineralized water during 24h) decreased their mineralization capacity (Fig. 7). The opposite result would have been expected to explain the discrepancy between the rankings obtained in the in vitro experiment and the in vivo studies (Table 6). It appears therefore likely that other factors than contaminants modulate the osteoinductive response, for example the resorbability [23,24] of the BGS (β-TCP vs HA and corresponding SSA) or physical features such as the topography [11, 12].

Bioactivity, described as the mineralization ability of BGS in SBF, has been traditionally used to test the osteoconductivity of biomaterials [14]. More recently, several authors [4,21,23] associated this property with osteoinduction. Nonetheless, it was not a mean to explain the mechanism by which BGS are osteoinductive contrary to what Bohner and Miron proposed [26]. Furthermore, the method used to decipher whether a BGS was osteoinductive or not was only qualitative. In the present study, the quantitative measurements allowed for a statistical approach to classifying BGS based on their mineralization ability in SBF. The fact that the predictions of the present study allowed to identify osteoinductive BGS that were studied in different countries by different teams of researchers in different large animal species is a testimony that mineralization is likely to be the trigger of osteoinduction (Tables 1 and 7). To our knowledge, this is the first account of a direct correlation between a quantitative in vitro experiment and in vivo osteoinduction results.

SSA has been shown to be one of the most important features of osteoinductive BGS [9–12,39,47]. It was hypothesized that a higher SSA induced a higher protein adsorption in vivo, which in turn fostered bone formation [47]. However, a higher SSA also provides with more nucleation sites for calcium phosphates to precipitate from the supersaturated bodily fluid, thus influencing the mineralization ability. For materials with equivalent surface chemistry and macrostructure but different SSA, this standalone measurement might be able to provide enough information to classify the materials according to their osteoinductive potential (Table 6, Fig. 3). Bulk microporosity of the materials has also been shown to be correlated to BGS osteoinductivity [48], but to a lesser extent than SSA. In the present study, microporosity and osteoinductive potential were not correlated, even though all 4 osteoinductive materials have a high microporosity and fine micropores (Fig. 2; Tables 3 and 6). It should be noted that the SSA was sometimes correlated to micropore size [11,38] and amount [25], which may be misleading towards identifying microporosity as an influencing factor rather than surface area [1]. Generally, small micropores are associated with high microporosity in ceramics because of sintering densification. Consequently, BGS having different pore sizes but the same microporosity have an SSA order following that of the pore sizes, i.e. the one with the smallest pores having the largest SSA. Calcium and phosphate release tests are often performed in PBS to show that BGS can release these ions in vivo. Calcium and phosphate release are thermodynamically impossible in physiological (or close to) conditions for both HA and β-TCP since they both exhibit positive saturation index in bodily fluids. However a correlation was observed between a high calcium and phosphate release in SPS [21], which is not saturated towards HA and β-TCP, and the osteoinductive potential of the BGS tested. For materials possessing the same exact chemistry, such measurement is equivalent to a total surface area measurement and can be normalized to obtain the SSA. In contrast, if the chemistry varies this measurement might be misleading. To compare materials, it is beneficial to add a mineralization experiment to other physicochemical tests. A mineralization experiment as described here provides information on the osteoinductive behaviour, and allow a faster and more economical comparison of bone graft substitutes when compared to cell culture and in vivo assays.

5. Conclusion

Quantitative mineralization experiments allowed a discrimination between osteoinductive and non-osteoinductive BGS, but failed to rank their osteoinductive potential. BGS trace contaminants (Ca^{2+}, Mg^{2+}, H^{+}, OH^{-}, PO_4^{3-}) could be readily detected by performing leachable experiments. These contaminants affected the mineralization, but did not allow to explain the discrepancy in the ranking. The use of quantitative mineralization experiments might be useful to detect the osteoinductive capacity of BGS early in the development process, allowing to screen prototypes, optimize resources and reduce animal usage. The present work is a testimony that mineralization could be the trigger of osteoinduction. Nevertheless, the overall mechanism might involve other properties of the BGS such as topography and resorption rate.

Credit author statement

Yassine Maazouz: Conceptualization, Validation, Formal analysis, Investigation, Data curation, Writing, Review, Editing, Visualization, Project administration, Funding acquisition. Giacomo Chizzola: Formal analysis, Investigation. Nicola Doebelin: Data curation, Writing, Review, Editing. Marc Bohner: Validation, Resources, Writing, Review, Editing, Supervision, Project administration, Funding acquisition.

Declaration of competing interest

The authors declare that they have no known competing financial interests or personal relationships that could have appeared to influence the work reported in this paper.

Acknowledgements

The authors would like to thank the company Kuros Biosciences for providing the BGS used in the present study and for the scientific input provided by Huipin Yuan, Nathan Kucko, Joost De Bruijn and Florence De Groot. The help of Yves Viecelli for ICP-MS measurements is also acknowledged. This research was partly funded by Innosuisse through the grant 36104.1.

Appendix A. Supplementary data

Supplementary data to this article can be found online at https://doi.org/10.1016/j.biomaterials.2021.120912.

Data availability statement

The raw/processed data required to reproduce these findings cannot be shared at this time due to technical or time limitations.

References

[1] A.M.C. Barradas, H. Yuan, C.A. van Blitterswijk, P. Habibovic, Osteoinductive biomaterials: current knowledge of properties, experimental models and biological mechanisms, Eur. Cell. Mater. 21 (2011) 407–429, discussion 429.
[2] D.C. Lobb, B.R. DeGeorge, A.B. Chhabra, Bone graft substitutes: current concepts and future expectations, J. Hand Surg. Am. 44 (2019) 497–505.e2.
[3] A. Bow, D.E. Anderson, M. Dhar, Commercially available bone graft substitutes: the impact of origin and processing on graft functionality, Drug Metab. Rev. 51 (2019) 533–544.
[4] S. Fujibayashi, M. Neo, H.M. Kim, T. Kokubo, T. Nakamura, Osteoinduction of porous bioactive titanium metal, Biomaterials 25 (2004) 443–450.
[5] G.D. Winter, B.J. Simpson, Heterotopic bone formed in a synthetic sponge in the skin of young pigs, Nature 223 (1969) 88–90.
[6] H. Yuan, Z. Yang, Y. Li, X. Zhang, J.D. De Bruijn, K. De Groot, Osteoinduction by calcium phosphate biomaterials, J. Mater. Sci. Mater. Med. 9 (1998) 723–726.
[7] Z. Tang, X. Li, Y. Tan, H. Fan, X. Zhang, The material and biological characteristics of osteoinductive calcium phosphate ceramics, Regen. Biomater. 5 (2018) 43–59.
[8] G. Daculsi, R.Z. LeGeros, E. Nery, K. Lynch, B. Kerebel, Transformation of biphasic calcium phosphate ceramics in vivo: ultrastructural and physicochemical characterization, J. Biomed. Mater. Res. 23 (1989) 883–894.
[9] J. Zhang, X. Luo, D. Barbieri, A.M.C. Barradas, J.D. De Bruijn, C.A. Van Blitterswijk, H. Yuan, The size of surface microstructures as an osteogenic factor in calcium phosphate ceramics, Acta Biomater. 10 (2014) 3254–3263.
[10] A. Barba, A. Diez-Escudero, M. Espanol, M. Bonany, J.M. Sadowska, J. Guillem-Marti, C. Öhman-Mägi, C. Persson, M.-C. Manzanares, J. Franch, M.-P. Ginebra,

Impact of biomimicry in the design of osteoinductive bone substitutes: nanoscale matters, ACS Appl. Mater. Interfaces 11 (2019) 8818–8830.
[11] R. Duan, D. Barbieri, X. Luo, J. Weng, J.D. de Bruijn, H. Yuan, Submicron-surface structured tricalcium phosphate ceramic enhances the bone regeneration in canine spine environment, J. Orthop. Res. 34 (2016) 1865–1873.
[12] N.L. Davison, X. Luo, T. Schoenmaker, V. Everts, H. Yuan, F. Barrère-de Groot, J. D. de Bruijn, Submicron-scale surface architecture of tricalcium phosphate directs osteogenesis in vitro and in vivo, Eur. Cell. Mater. 27 (2014) 281–297.
[13] R. Duan, L.A. van Dijk, D. Barbieri, F. de Groot, H. Yuan, J.D. de Bruijn, Accelerated bone formation by biphasic calcium phosphate with a novel sub-micron surface topography, Eur. Cell. Mater. 37 (2019) 60–73.
[14] T. Kokubo, H. Takadama, How useful is SBF in predicting in vivo bone bioactivity? Biomaterials 27 (2006) 2907–2915.
[15] T. Kitsugi, T. Yamamuro, T. Nakamura, T. Kokubo, M. Takagi, T. Shibuya, H. Takeuchi, M. Ono, Bonding behavior between two bioactive ceramics in vivo, J. Biomed. Mater. Res. 21 (1987) 1109–1123.
[16] C. Zhao, X. Zhu, K. Liang, J. Ding, Z. Xiang, H. Fan, X. Zhang, Osteoinduction of porous titanium: a comparative study between acid-alkali and chemical-thermal treatments, J. Biomed. Mater. Res. B Appl. Biomater. 95 B (2010) 387–396.
[17] T. Kawai, M. Takemoto, S. Fujibayashi, H. Akiyama, M. Tanaka, S. Yamaguchi, D. K. Pattanayak, K. Doi, T. Matsushita, T. Nakamura, T. Kokubo, S. Matsuda, Osteoinduction on acid and heat treated porous Ti metal samples in canine muscle, PloS One 9 (2014) 1–10.
[18] M. Takemoto, S. Fujibayashi, M. Neo, J. Suzuki, T. Matsushita, T. Kokubo, T. Nakamura, Osteoinductive porous titanium implants: effect of sodium removal by dilute HCl treatment, Biomaterials 27 (2006) 2682–2691.
[19] A.K. Miri, N. Muja, N.O. Kamranpour, W.C. Lepry, A.R. Boccaccini, S.A. Clarke, S. N. Nazhat, Ectopic bone formation in rapidly fabricated acellular injectable dense collagen-Bioglass hybrid scaffolds via gel aspiration-ejection, Biomaterials 85 (2016) 128–141.
[20] P. Habibovic, In vitro and in vivo bioactivity assessment of a polylactic acid/ hydroxyapatite composite for bone regeneration, Biomatter 4 (2014), e27664.
[21] R. Duan, D. Barbieri, X. Luo, J. Weng, C. Bao, J.D. De Bruijn, H. Yuan, Variation of the bone forming ability with the physicochemical properties of calcium phosphate bone substitutes, Biomater. Sci. 6 (2018) 136–145.
[22] J.Y. Chen, Y.R. Duan, C.L. Deng, Q.Y. Zhang, X.D. Zhang, A comparative study between dynamic and static simulated body fluid methods, Key Eng. Mater. 309–311 (2006) 271–274.
[23] Z. Tang, X. Li, Y. Tan, H. Fan, X. Zhang, The material and biological characteristics of osteoinductive calcium phosphate ceramics, Regen. Biomater. 5 (2018) 43–59.
[24] A. Barba, A. Diez-Escudero, Y. Maazouz, K. Rappe, M. Espanol, E.B. Montufar, M. Bonany, J.M. Sadowska, J. Guillem-Marti, C. Öhman-Mägi, C. Persson, M.-C. Manzanares, J. Franch, M.-P. Ginebra, Osteoinduction by foamed and 3D-printed calcium phosphate scaffolds: effect of nanostructure and pore architecture, ACS Appl. Mater. Interfaces 9 (2017) 41722–41736.
[25] P. Habibovic, H. Yuan, C.M. van der Valk, G. Meijer, C.A. van Blitterswijk, K. de Groot, 3D microenvironment as essential element for osteoinduction by biomaterials, Biomaterials 26 (2005) 3565–3575.
[26] M. Bohner, R.J. Miron, A proposed mechanism for material-induced heterotopic ossification, Mater. Today 22 (2019) 132–141.
[27] Technical Committee ISO/TC 150, INTERNATIONAL STANDARD ISO 23317 : Implants for Surgery — in Vitro Evaluation for Apatite-Forming Ability of Implant Materials, Second Ed. 2012-10-01. 2007, 2014, p. 13.
[28] W. Zhao, D. Michalik, S. Ferguson, W. Hofstetter, J. Lemaître, B. von Rechenberg, P. Bowen, Rapid evaluation of bioactive Ti-based surfaces using an in vitro titration method, Nat. Commun. 10 (2019).
[29] Y. Maazouz, I. Rentsch, B. Lu, B. Le Gars Santoni, N. Doebelin, M. Bohner, In vitro measurement of the chemical changes occurring within β-tricalcium phosphate bone graft substitutes, Acta Biomater. 102 (2020) 440–457.
[30] L. Lin, K.L. Chow, Y. Leng, Study of hydroxyapatite osteoinductivity with an osteogenic differentiation of mesenchymal stem cells, J. Biomed. Mater. Res. 89A (2009) 326–335.
[31] Y.C. Chai, S.J. Roberts, J. Schrooten, F.P. Luyten, Probing the osteoinductive effect of calcium phosphate by using an in vitro biomimetic model, Tissue Eng. 17 (2011) 1083–1097.
[32] C. Seebach, J. Schultheiss, K. Wilhelm, J. Frank, D. Henrich, Comparison of six bone-graft substitutes regarding to cell seeding efficiency, metabolism and growth behaviour of human mesenchymal stem cells (MSC) in vitro, Injury 41 (2010) 731–738.
[33] A. Kübler, J. Neugebauer, J.-H. Oh, M. Scheer, J.E. Zöller, Growth and proliferation of human osteoblasts on different bone graft substitutes an in vitro study, Implant Dent. 13 (2004) 171–179.
[34] P. Habibovic, T. Woodfield, K. De Groot, C. Van Blitterswijk, Predictive value of in vitro and in vivo assays in bone and cartilage repair - what do they really tell us about the clinical performance? Adv. Exp. Med. Biol. 585 (2006) 327–360.
[35] G. Hulsart-Billström, J. Dawson, S. Hofmann, R. Müller, M. Stoddart, M. Alini, R. Redl, A. El Haj, R. Brown, V. Salih, J. Hilborn, S. Larsson, R. Oreffo, A surprisingly poor correlation between in vitro and in vivo testing of biomaterials for bone regeneration: results of a multicentre analysis, Eur. Cell. Mater. 31 (2016) 312–322.
[36] Z. Yang, H. Yuan, W. Tong, P. Zou, W. Chen, X. Zhang, Osteogenesis in extraskeletally implanted porous calcium phosphate ceramics: variability among different kinds of animals, Biomaterials 17 (1996) 2131–2137.
[37] Z.J. Yang, H.P. Yuan, P. Zou, W.D. Tong, S.X. Qu, X.D. Zhang, Osteogenic responses to extraskeletally implanted synthetic porous calcium phosphate ceramics: an early stage histomorphological study in dogs, J. Mater. Sci. Med. 8 (1997) 697–701.
[38] H. Yuan, H. Fernandes, P. Habibovic, J. de Boer, A.M. Barradas, A. de Ruiter, W. R. Walsh, C.A. van Blitterswijk, J.D. de Bruijn, Osteoinductive ceramics as a synthetic alternative to autologous bone grafting, Proc. Natl. Acad. Sci. U. S. A. 107 (2010) 13614–13619.
[39] N.L. Davison, J. Su, H. Yuan, J.J.J.P. van den Beucken, J.D. de Bruijn, F.B. de Groot, Influence of surface microstructure and chemistry on osteoinduction and osteoclastogenesis by biphasic calcium phosphate discs, Eur. Cell. Mater. 29 (2015) 314–329.
[40] N. Doebelin, R. Kleeberg, Profex: a graphical user interface for the Rietveld refinement program BGMN, J. Appl. Crystallogr. 48 (2015) 1573–1580.
[41] K. Sudarsanan, R.A. Young, Significant precision in crystal structure details: holly springs hydroxyapatite, Acta Crystallogr. B25 (1969) 1534–1543.
[42] L.W. Schroeder, B. Dickens, W.E. Brown, Crystallographic studies of the role of Mg as a stabilizing impurity in β-Ca3(PO4)2. II. Refinement of Mg-containing β-Ca3 (PO4)2, J. Solid State Chem. 22 (1977) 253–262.
[43] V.G. Tsirelson, A.S. Avilov, Y.A. Abramov, E.L. Belokoneva, R. Kitaneh, D. Feil, X-ray and electron diffraction study of MgO, Acta Crystallogr. Sect. B Struct. Sci. 54 (1998) 8–17.
[44] A. Tharwat, Classification assessment methods, Appl. Comput. Informatics 17 (1) (2021) 168–192, https://doi.org/10.1016/j.aci.2018.08.003.
[45] M. Li, X. Guo, W. Qi, Z. Wu, J.D. de Bruijn, Y. Xiao, C. Bao, H. Yuan, Macrophage polarization plays roles in bone formation instructed by calcium phosphate ceramics, J. Mater. Chem. B. 8 (2020) 1863–1877.
[46] N. Doebelin, Y. Maazouz, R. Heuberger, M. Bohner, A.A. Armstrong, A.J. Wagoner Johnson, C. Wanner, A thermodynamic approach to surface modification of calcium phosphate implants by phosphate evaporation and condensation, J. Eur. Ceram. Soc. (2020).
[47] X.D. Zhu, H.S. Fan, Y.M. Xiao, D.X. Li, H.J. Zhang, T. Luxbacher, X.D. Zhang, Effect of surface structure on protein adsorption to biphasic calcium-phosphate ceramics in vitro and in vivo, Acta Biomater. 5 (2009) 1311–1318.
[48] D. Le Nihouannen, G. Daculsi, A. Saffarzadeh, O. Gauthier, S. Delplace, P. Pilet, P. Layrolle, Ectopic bone formation by microporous calcium phosphate ceramic particles in sheep muscles, Bone 36 (2005) 1086–1093.
[49] M. Bohner, J. Lemaitre, Can bioactivity be tested in vitro with SBF solution? Biomaterials 30 (2009) 2175–2179.